Bone Regrowth After Frontal Burr Hole Craniostomy: Natural History of 14-mm and 20-mm Burr Holes and Implications for Postoperative Trans-Burr Hole Ultrasound

Albert Antar, BS, Ryan P. Lee, MD, Shahab Aldin Sattari, MD, Michael Meggyesy, MD, Jheesoo Ahn, BSN, Carly Weber-Levine, MS, Kelly Jiang, MS, Judy Huang, MD, Mark Luciano, MD, PhD

Department of Neurosurgery, Johns Hopkins University School of Medicine, Baltimore, Maryland, USA

Previously presented at Congress of Neurological Surgeons Annual Meeting in San Franciso, CA from October 8 to 12, 2022; and at the Hydrocephalus Meeting in Hamburg, Germany from August 25 to 28, 2023.

Correspondence: Mark Luciano, MD, PhD, Department of Neurosurgery, Johns Hopkins Hospital, 600 N. Wolfe St Phipps Suite 126, Baltimore, MD 21287, USA.
Email: markluciano@jhmi.edu

Received, April 16, 2024; **Accepted,** June 19, 2024; **Published Online,** September 10, 2024.

Neurosurgery Practice 2024;5(4):e00110. https://doi.org/10.1227/neuprac.0000000000000110

BACKGROUND AND OBJECTIVE: Burr hole craniostomy is performed for ventriculoperitoneal shunt insertion and endoscopic third ventriculostomy in patients with cerebrospinal fluid disorders. These burr holes are increasingly being used as windows for postoperative ultrasound, an investigational alternative to computed tomography or MRI for follow-up imaging of ventricular caliber. However, bone regrowth reduces ultrasound visibility, and little is known about burr hole regrowth rates in adults. Our study evaluates burr hole regrowth patterns and implications for transcranial ultrasound imaging.

METHODS: We retrospectively analyzed 101 consecutive patients who had frontal burr hole craniostomy for new ventriculoperitoneal shunt insertion or endoscopic third ventriculostomy over a 3-year period. A mix of standard 14-mm burr holes and expanded 20-mm burr holes were used. Burr hole bone regrowth was assessed using serial follow-up computed tomography scans. Linear and logistic regression analyses examined if bone regrowth correlated with any clinical variables.

RESULTS: There was wide variability in rate and degree of burr hole regrowth. The average percentage closure was 25% at 6 months, with minimal additional closure over the following 18 months. The mean residual diameter for 14-mm and 20-mm burr holes stabilized around 9.4 mm and 15.4 mm, respectively. Bone regrowth was not associated with patient characteristics, including age, sex, skull thickness, or etiology of cerebrospinal fluid disorder. Rate of bone regrowth was similar between both cohorts.

CONCLUSION: Bone regrowth after burr hole craniostomy is common, even in elderly patients, occurring rapidly within the first 6 to 12 months and subsequently stabilizing. It is frequently severe enough to restrict ultrasound visualization. Regrowth could not be predicted with any investigated variables, so uniform techniques are needed to block regrowth to allow for longitudinal ultrasound imaging, such as full-thickness cylindrical burr hole implants.

KEY WORDS: Bone regrowth, Cranioplasty, Imaging, Sonolucent, Ultrasound

Management of patients with hydrocephalus and cerebrospinal fluid (CSF) disorders necessitates longitudinal imaging, typically involving repeat computed tomography (CT) or MRI.[1] CT poses cumulative radiation risk, and MRI is expensive.[2,3] Unlike in infants, where open fontanelles allow for ultrasound-based brain and ventricular imaging,[4] the use of ultrasound for anatomic imaging of intracranial contents in older children and adults has traditionally been precluded by an intact calvarium.[5] However, many recent reports have demonstrated feasibility of transcranial imaging through sonolucent cranioplasty

ABBREVIATIONS: ETV, endoscopic third ventriculostomy; **PMMA,** polymethyl methacrylate; **VP,** ventriculoperitoneal.

materials, such as polymethyl methacrylate (PMMA). In this setting, transcranioplasty ultrasound provides a cost-effective, radiation-free, point-of-care alternative to other imaging modalities.[6-9] Specifically, our group has shown that ultrasound of the ventricular system can be performed postoperatively through PMMA burr hole covers in ventricular shunt and endoscopic third ventriculostomy (ETV) patients.

The value of trans-burr hole ultrasound in patients with hydrocephalus is predicated on the ability of ultrasound to be performed to monitor ventricular caliber longitudinally. Given that the ultrasound window through a burr hole is already limited, any significant bone regrowth would thus further constrain the view of the ultrasound. To our knowledge, there are no prior reports in the literature on frequency and rate of burr hole regrowth in adults. In this study, we examine rate of burr hole regrowth in adult patients with hydrocephalus. The first group analyzed are patients with standard 14-mm perforator (Acra-cut) burr holes and no burr hole cover. The second group are patients with expanded 20-mm burr holes with a sonolucent PMMA burr hole cover, placed to allow for trans-burr hole ultrasound imaging. For both groups, the rates and degree of burr hole regrowth as well as predictors for regrowth are reported. Implications for trans-burr hole ultrasound are discussed.

METHODS

Study Population and Surgical Technique

The study was reviewed by the Johns Hopkins Medical Institutional Review Board and qualified as exempt research under Department of Health and Human Services (DHHS) regulations. Records were reviewed for all consecutive adult (>/= 18 years of age) patients who underwent first time ventriculoperitoneal (VP) shunt and ETV by the senior author between September 1, 2019, and August 3, 2022. Only 14-mm burr holes were used until September 2020, at which point 20-mm burr holes became the standard for the purpose of trans-burr hole ultrasound postoperatively. Charts were reviewed retrospectively between December 2022 and June 2023. Patients were required to have at least 1 immediate postoperative head CT scan while admitted and at least 1 follow-up CT scan of the head after discharge from the initial surgical encounter.

For both groups, initial burr holes were created at Kocher's point with a 14-mm perforator bit (Acra-cut). In the 14-mm burr hole group, no further modifications were made and the procedure was performed through this burr hole. In the 20-mm burr hole cohort, the initial 14-mm burr hole was widened to 20 mm using a 4-mm round cutting burr to enable a wider ultrasound field of view. VP shunt insertion or ETV was then performed in the standard fashion. Particular consideration was given to ensure that the burr hole was cylindrical and that the inner cortex was rongeured to make the edges straight. Nothing additional was performed to the bone edges, except standard bone wax application for hemostasis as needed. The dura was not closed in either group. Patients undergoing ETV had a piece of gel foam placed under the burr hole cover. For the 20 mm group, an FDA-approved, off-the-shelf 2-cm (diameter) sonolucent PMMA implant (ClearFit®, Longeviti) was then used to reconstruct the burr hole and fixated to the skull using a standard cranial titanium plating system. Burr hole cover thickness was either 3.4 mm or 5.4 mm at the discretion of the surgeon.

In addition to routine imaging with CT and MRI per standard of care, patients in the 20-mm burr hole group underwent transcutaneous ultrasound with a GE Venue GO point-of-care system using a 3Sc probe for the evaluation of ventricle size throughout their follow-up period. Institutional Review Board approval was obtained for review and analysis of clinical and radiologic data. Need for individual patient consent to retrospectively abstract clinical and radiographic data was waived. Variables included age, sex, etiology, skull thickness, implant size, and burr hole diameter at the initial and each follow-up CT scan.

Analysis

Statistical analysis was performed using Stata (version 17.0, statacorp) and R Studio (Version 4.1.2., The R Foundation). Statistical significance was set at $P < .05$. For measurement and study of burr hole regrowth, orthogonal multiplanar reconstructions were created from the head CT scans at each time point and the study team measured the smallest diameter at all time points. Burr hole closure was calculated by measuring the smallest observed diameter on follow-up imaging and dividing that measurement by the initial burr hole diameter. Gantry was controlled for by selecting orthogonal cross-sectional images in which the entirety of the burr hole was in view and at its widest. Skull thickness was measured as an average of the bone thickness on either side of the burr hole on the reconstructed image. Burr hole closure (proportion of burr hole diameter at last follow-up compared to initial diameter) was plotted over time. Burr hole bone regrowth for both cohorts were plotted using Excel (Version 16.7, Microsoft) from the initial CT scan to the first follow-up CT scan. A line of best fit was applied to the plots. Linear, exponential, and logarithmic fits were trialed. To statistically compare the fitted models and ascertain if there were significant differences between the 2 cohorts' burr hole closure rates over time, a bootstrap analysis with 1000 resamples was conducted. This analysis generated empirical distributions of the differences in the intercepts of the logarithmic models fitted to each cohort's data, thereby allowing for the estimation of 95% confidence intervals for these differences.

Linear regression was performed correlating burr hole window closure to patient age, sex, implant size (20-mm cohort only), and skull thickness. Logistic regression was performed correlating the burr hole window closure to etiology of hydrocephalus (idiopathic intracranial hypertension, obstructive hydrocephalus, congenital hydrocephalus, and communicating hydrocephalus) using normal pressure hydrocephalus as a reference.

RESULTS

We identified 101 total patients who met inclusion criteria: 39 patients who underwent 14-mm burr hole craniostomy and 62 patients who underwent 20-mm burr hole craniostomy. Baseline characteristics were not significantly different (Table 1), except follow-up time was longer in the 14 mm group due to the delayed implementation of the 20 mm technique in the study period. Overall mean follow-up time was 347.2 days: 622.5 days in the 14 mm group and 242.7 days in the 20 mm group. The mean age for the 14 mm cohort was 59.1 years (range 19-90) and 65.5 years (range 21-85) for the 20 mm cohort. Overall mean age was 63.1 years (range 19-90). The most common etiology was normal pressure hydrocephalus (74/101, 73%).

TABLE 1. Study Demographics

Patient Characteristics	All patients	14 mm cohort	20 mm cohort	*P*
No. of patients	101	39	62	
Age, mean (SD)	63.1 (18)	59.1 (19.5)	65.5 (16.7)	.088
Gender, N (%)				
Female	50 (50)	22 (56)	28 (45)	.271
Male	51 (50)	17 (44)	34 (55)	
Follow-up days, mean (SD)	347.2 (323.8)	622.5 (341.8)	242.7 (198.4)	<.001
Etiology				
NPH	74	24	50	
IIH	13	7	6	
Obstructive hydrocephalus	4	2	2	
Congenital hydrocephalus	5	1	4	
CSF leak	1	1	0	
Venous thrombosis	2	2	0	
TBI	1	1	0	
LOVA	1	1	0	.123

CSF, cerebrospinal fluid; IIH, idiopathic intracranial hypertension; LOVA, longstanding overt ventriculomegaly of adulthood; NPH, normal pressure hydrocephalus; TBI, traumatic brain injury.

Demographic data summarized for all patients, then subdivided into the 14 mm and 20 mm cohorts. Patient characteristics including age, gender, and etiology are not statistically different between both cohorts. The mean follow-up time is significantly less in the 20 mm cohort because this technique was not used until 1 year into the study period.

There was wide variability in rate and degree of burr hole regrowth cumulatively and within each cohort (Figure 1). Burr hole regrowth demonstrated a logarithmic pattern, with a faster rate of regrowth early followed by a plateau. The mean percentage closure was 25% at 6 months, stabilizing slightly higher around 26% at 12 and 24 months (Table 2). When looking at just 14-mm burr holes, the mean percentage closure was approximately 30-32% at 6 months and beyond. In the 20 mm cohort, the burr holes had decreased in diameter an average of 21% at 6 months and then leveled out at 23% at 12 and 24 months. The absolute mean bone regrowth between both cohorts was similar at 6 months, 1 year, and 2 years as demonstrated in Table 2. Bootstrap analysis revealed that there was no statistical difference in the intercepts and slopes of the logarithmic models when applied to the 2 cohorts. This indicates that the rates of burr hole closure over time did not differ between the 14 mm and 20 mm cohorts.

Representative reconstructed head CT images orthogonal to the frontal burr hole are shown in Figure 2. In all cases, the pattern of regrowth was from the bone edges, rather than from dura, in-pointed and triangular pattern from the mid-depth. Bone regrowth involved the cancellous layer and both the inner and outer cortex in all patients. The implant did prevent bone regrowth superficially at its site of contact with the bone edges, but the implant did not penetrate deep enough in the burr hole to prevent overall bone regrowth, which occurred below it. Figure 3 shows a representative case wherein burr hole regrowth narrows the cone of visualization of ventricular ultrasound at longitudinal post-operative time points. Similarly, degree of regrowth correlated appropriately with expected visualization on US. The 14-mm burr holes tapered to a mean diameter of 9.5 mm at 6 months and then only slightly smaller for the next 18 months before stabilizing (Table 2). The 20-mm burr holes reduced in diameter to 15.8 mm at 6 months and then stabilized at 15.4 mm, which, as the example in Figure 3 shows, is still sufficient for visualization, albeit less ideal.

Although there was high variability, the degree of regrowth was notable and clinically significant in affecting visualization. Therefore, we next looked at predictors of regrowth pattern. For the cumulative group, linear regression similarly did not demonstrate any correlation between burr hole window closure and age (P = .47), sex (P = .77), or skull thickness (P = .69) in all patients (Table 3A). In the 14 mm cohort, linear regression also did not demonstrate any correlation between burr hole window closure and age (P = .14), sex (P = .90), or skull thickness (P = .20) (Table 3B). In the 20 mm cohort, linear regression demonstrated no correlation between burr hole window closure and age

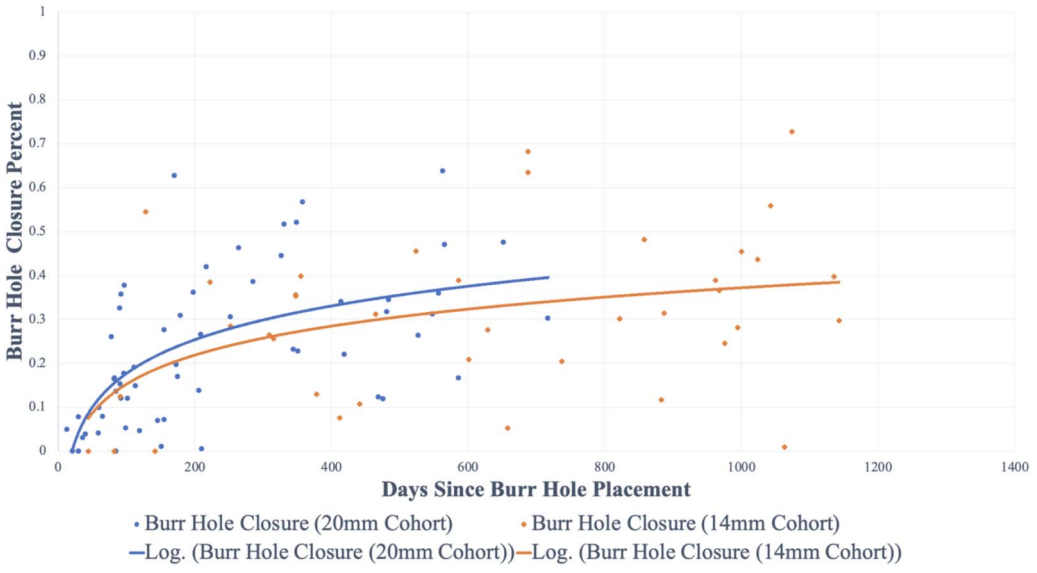

FIGURE 1. *Burr hole closure vs time burr hole window closure over time for all patients. Data points represent percentage of closure of burr hole diameter on most recent CT scan relative to the immediate postoperative CT scan.*

(P = .73), sex (P = .74), skull thickness (P = .93), or implant size (P = 1.00) (Table 3C).

Regarding etiology of CSF disorder in both cohorts, logistic regression did not demonstrate any correlation between the burr hole window closure and etiology of hydrocephalus using normal pressure hydrocephalus as a reference (Table 4A and 4B). Logistic regression similarly did not demonstrate any correlation between the burr hole window closure and etiology of hydrocephalus using normal pressure hydrocephalus as a reference in all patients (Table 4C). Although most patients had a diagnosis of normal pressure hydrocephalus, this was unlikely to act as a confounder given a lack of association between age or etiology of hydrocephalus with bone regrowth.

DISCUSSION

Patients with hydrocephalus or other CSF disorders require serial radiographic evaluation after surgical intervention.[1] One such component is the evaluation of ventricular caliber by CT or magnetic resonance–based imaging. Repeat CT, however, carries cumulative radiation risk, and serial MRI is expensive.[2,3] Transcranial ultrasound has been demonstrated to be feasible for monitoring ventricular caliber after ETV or VP shunt insertion in patients implanted with a sonolucent cover after burr hole craniostomy.[5] Under this treatment paradigm, patients are implanted with a sonolucent cover after burr hole craniostomy, allowing ultrasound imaging to be performed point of care by the neurosurgical team during follow-up appointments. This approach offers several benefits: no radiation exposure, reduced cost compared with CT or MRI, immediate results that can be discussed with the patient during the same visit, and potential financial compensation for neurosurgeons, as opposed to revenue typically captured by radiology departments. However, there are limitations, including the higher cost of sonolucent burr hole covers and the necessity for additional training to accurately perform and interpret transcranial ultrasound, which is operator-dependent. In addition, further studies are needed to determine the sensitivity and specificity of this imaging modality compared with established techniques such as CT and MRI. Despite these challenges, transcranial ultrasound through sonolucent burr hole covers offers a promising alternative to traditional imaging methods, warranting further research and consideration in clinical practice.

The utility of follow-up radiographic evaluation with ultrasound is contingent on the burr hole window. An open burr hole, without significant bone regrowth, is therefore critical to enable ultrasound to act as a reasonable imaging alternative to CT or MRI for patients with hydrocephalus or other CSF disorders. Anecdotally, burr holes in children and young adults are known to often have bony ingrowth. Burr holes made for ventricular catheter implantation often are observed to regrow almost completely on long-term follow-up. However, there are no reports on the rate or frequency of this process. Bone regrowth is also less commonly observed in older adults, and there is no published data on whether there is appreciable bone regrowth in that age group at all.

Bone Regrowth

To our knowledge, our study is the first to quantitate bone regrowth in a large cohort of adult patients after burr hole

TABLE 2. Temporal Trends in Percent Closure and Residual Size: Residual Burr Hole Diameter was Measured on All Follow-up CT Scans at Each 6-Month, 1-Year, and 2-Year Time Points

Follow-up Interval	All patients	14 mm burr hole	20 mm burr hole
6 months			
Percent closure			
25th percentile	12%	15%	7%
Mean	25%	32%	21%
75th Percentile	36%	45%	33%
Residual diameter			
25th percentile	—	11.9 mm	18.6 mm
Mean	—	9.5 mm	15.8 mm
75th percentile	—	7.7 mm	13.4 mm
1 year			
Percent closure			
25th percentile	12%	15%	8%
Mean	26%	31%	23%
75th percentile	38%	43%	35%
Residual diameter			
25th percentile	—	11.9 mm	18.4 mm
Mean	—	9.7 mm	15.4 mm
75th percentile	—	8.0 mm	13.0 mm
2 years			
Percent closure			
25th percentile	12%	13%	8%
Mean	26%	30%	23%
75th percentile	38%	40%	35%
Residual diameter			
25th percentile	—	12.2 mm	18.4 mm
Mean	—	9.8 mm	15.4 mm
75th percentile	—	8.4 mm	13.0 mm

These results were used to calculate 25th percentile, mean, and 75th percentile percent closure from original and absolute residual diameter.

craniostomy. Bone regrew from the edges of the burr hole rapidly (within the first 6-12 months) and tapered toward a single point, after which bone regrowth was minimal. Bone regrowth never completely closed the defect in any patient observed during the study period but rather, partially obscured the opening, decreasing the field of view for ultrasound. This pattern was consistent for 14-mm and 20-mm starting sizes. Bone regrowth was not associated with any patient characteristic including age, gender, or skull thickness for either cohort. The patients with 20-mm burr holes had either 3.4-mm or 5.4-mm thick PMMA burr hole covers placed. These were placed such that up to 1 to 2 mm was proud above the outer table, and the remaining thickness of the implant protruded into the burr hole. There was no difference in the rate and degree of burr hole regrowth in the thicker or thinner sizes. This is likely because the bone thickness at the frontal location is often 10 mm or larger. Thicker implants, which cover the full thickness of bone, may mechanically prevent bone regrowth, and this should be investigated in future research.

Proposed Mechanism

Prior research proposes 3 potential mechanisms for calvarial bone regrowth.[10] First, dormant osteoblasts in the periosteum may become active after bone fractures.[11] Second, dural contact could enhance osteogenesis.[12,13] Last, the diploë from adjacent bone may supply osteogenic cells that contribute to new bone formation.[14] Inflammation may further stimulate osteogenesis by promoting neovascularization, which in turn encourages bone regrowth and survival.[15]

A potential mechanism explaining the regrowth pattern observed in our study is that bone regeneration may be primarily driven by osteogenesis originating from remnants of bone dust and augmented by inflammatory neovascularization. The likelihood of dural osteogenesis is minimal, as the dura was not repaired in either cohort. Similarly, osteogenesis from the adjacent diploë is improbable due to the use of bone wax for hemostasis. Further research should explore the mechanism behind bone regrowth in this patient population.

Implications for Transcranial Ultrasound in Adult Populations

To date, multiple studies, including several by our group, have demonstrated the safety and feasibility of transcranial ultrasound using sonolucent PMMA material.[6,8,9,16-18] Belzberg et al[9] demonstrated the feasibility of sonolucent cranioplasty after decompressive hemicraniectomy. Flores et al and Salem et al both demonstrated the potential for sonolucent cranioplasty in extracranial-intracranial bypass procedures.[16,17] In both studies, ultrasound agreed with computed tomography angiography regarding bypass patency in all patients (32) studied. Del Bene et al[18] investigated the use of sonolucent cranioplasty after the removal of an oligodendroglioma and illustrated the ability of ultrasound to note recurrence of tumor at 30 months postoperatively in agreement with MRI. O'Malley et al outlined the substantial cost savings procured by the use of transcranial

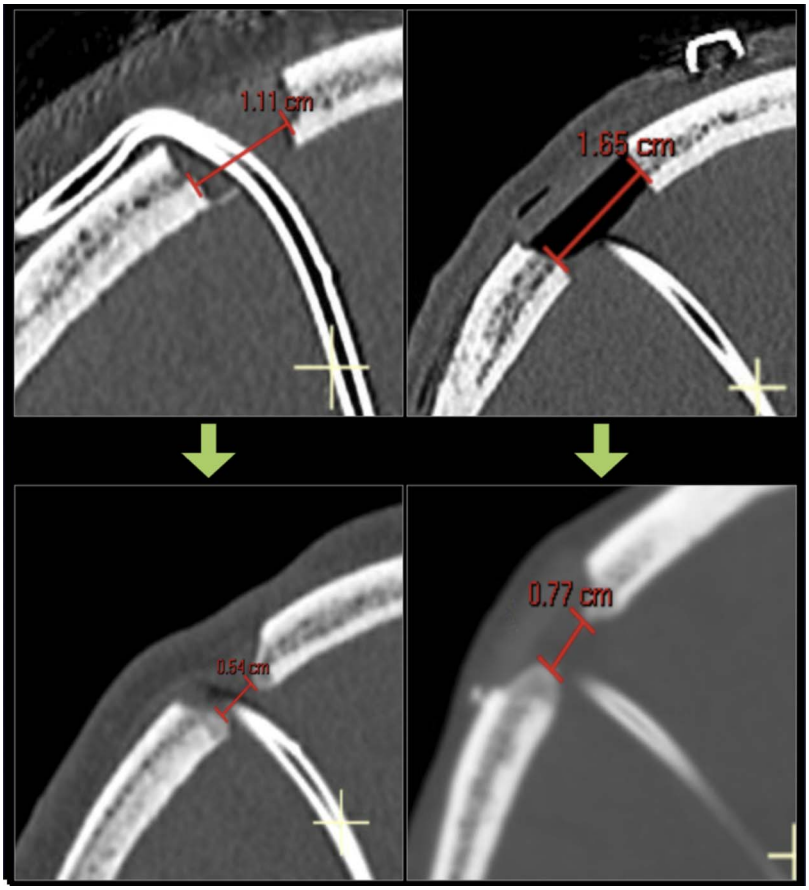

FIGURE 2. *Representative head CT scans after burr hole craniostomy. Top left panel is a reconstructed immediate postoperative head CT scan showing a 14-mm burr hole created by the perforator bit. Bottom left panel is a follow-up reconstructed CT scan in the same patient with bony regrowth down to a diameter of 5.4 mm. The top right panel represents a patient with a 20-mm burr hole immediately postoperative, and the bottom right shows a follow-up CT scan in the same patient with regrowth down to 7.7 mm. Note that original burr hole sizes are often less than intended due to tapering at the depth.*

ultrasound in patients implanted with sonolucent material at approximately $2000 to 4500 over several follow-up visits.[19] No study, however, has delineated how bone regrowth may affect the feasibility of transcranial ultrasound for long-term follow-up. As demonstrated, bone regrowth occurs in nearly all patients after burr hole craniostomy, and although its rate is fairly predictable in a large cohort of patients, it is highly variable in individual patients. We also illustrated that this bone regrowth is clinically significant, as it may affect ultrasound field of view. Developing novel techniques to address bone regrowth will be essential. Potential approaches include using wider burr holes, encasing burr hole edges, rigorously washing the operative site to remove residual bone dust, or implementing full-thickness sonolucent implants. These measures are necessary if transcranial ultrasound is to become a viable alternative to other imaging modalities in the neurosurgical context.

Limitations

Our study provides first evidence of frequent bone regrowth in adults after burr hole craniostomy. However, it has limitations. Our study cohort was relatively small, which limited our ability to investigate associations between comorbidities and medications on bone regrowth. Despite this, bone regrowth was frequent; future research should investigate whether comorbidities and medications affect bone regrowth. Another limitation was our inability to compare sonolucent cranioplasty across similar burr hole diameters. In addition, limited

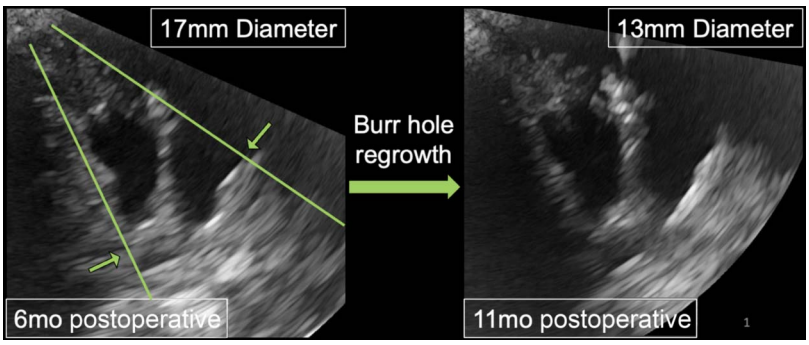

FIGURE 3. *Representative postoperative trans-burr hole ultrasound images through a fontal burr hole showing cross sections of the lateral and third ventricles in the coronal plane. The left panel is an ultrasound image 6 months after 20-mm burr hole craniostomy for ventriculoperitoneal shunt placement, with a residual burr hole size of 17 mm. The green lines represent the decreased field of view, shown in the right panel, available for ultrasound secondary to bone regrowth down to a residual burr hole size of 13 mm at 11 months postoperatively.*

implant size variability restricted comparisons between thicker and thinner implants' impact on regrowth. Moreover, while visual inspections of regrowth sources were possible, layer-specific analyses were not performed. Finally, with only 2-to-3 years of follow-up, long-term conclusions remain limited. Still, data suggest regrowth ceases after the initial 6 to 12 months.

TABLE 3. Linear Regression was Performed Correlating Burr Hole Closure to Age, Sex, and Skull Thickness, for (A) All Patients, (B) Patients in the 14 mm Cohort, (C) Patients in the 20 mm Cohort

Variable	Regression coefficient	95% CI	*P* value
(A) All burr hole closure[a]			
Age	1.000	0.996-1.002	.47
Sex	0.985	0.889-1.092	.77
Skull thickness (mm)	1.004	0.981-1.030	.69
(B) 14 mm burr hole closure[a]			
Age	0.997	0.993-1.001	.14
Sex	1.010	0.854-1.196	.90
Skull thickness (mm)	1.035	0.981-1.092	.20
(C) 20 mm burr hole closure[a]			
Age	1.001	0.997-1.005	.73
Sex	0.977	0.852-1.120	.74
Skull thickness (mm)	0.999	0.971-1.027	.93
Implant size (mm)	1.000	0.937-1.067	1.00

[a]Standardized by follow-up time.
Results were standardized by follow-up time. No variable was statistically significant.

TABLE 4. Univariable Logistic Regression was Performed Correlating Burr Hole Window Closure to Etiology Using Normal Pressure Hydrocephalus as a Reference, for (A) All Patients, (B) Patients in the 14 mm Cohort, (C) Patients in the 20 mm Cohort

Etiology[a]	Odds ratio (95% CI)	*P*
(A)		
Idiopathic intracranial hypertension	0.961 (0.555-1.426)	.95
Obstructive hydrocephalus	1.121 (0.196-6.423)	.89
Congenital hydrocephalus[b]	<0.001	.99
Communicating hydrocephalus	0.561 (0.025-6.112)	.64
Venous thrombosis[b]	>1	.99
TBI[b]	>1	.99
(B)		
Idiopathic intracranial hypertension	1.111 (0.198-6.784)	.90
Obstructive hydrocephalus	1.667 (0.139-39.034)	.69
(C)		
Idiopathic intracranial hypertension	0.643 (0.083-3.627)	.63
Obstructive hydrocephalus	0.643 (0.029-7.155)	.73
Congenital hydrocephalus[b]	<0.001	.99
Communicating hydrocephalus	1.286 (0.049-33.806)	.86

[a]Reference point is normal pressure hydrocephalus.
[b]CI was not reported given extremely large range encompassing infinity.
No variable was statistically significant.

CONCLUSION

Our study indicates that bone regrowth after burr hole craniostomy is common. Regrowth is rapid within the first 6 to 12 months after surgery after which point bone regrowth ceases. Although we demonstrated that bone regrowth is not correlated with patient age, sex, skull thickness, diagnosis, or implant size, it is unclear which factors explain why some patients experience more profound regrowth than others and future research should aim to elucidate this. A consistent pattern of bone regrowth across patients translates to a decreased ultrasound field of view for follow-up–based imaging in patients undergoing VP shunt insertion or ETV for hydrocephalus or other CSF disorders, particularly 1 year postoperatively. New techniques and materials, such as full-thickness sonolucent implants, are needed to enable ultrasound to act as a viable alternative to CT or MRI for long-term imaging in this patient population.

Funding

This study did not receive any funding or financial support.

Disclosures

Under a licensing agreement between Longeviti Neuro Solutions, LLC, and the Johns Hopkins University, the university is entitled to royalty distributions on technologies described in this publication. This arrangement has been reviewed and approved by the Johns Hopkins University in accordance with its conflict-of-interest policies. Judy Huang is a stockholder in Longeviti Neuro Solutions. Judy Huang and Mark Luciano are consultants for Longeviti Neuro Solutions. The other authors have no personal, financial, or institutional interest in any of the drugs, materials, or devices described in this article.

REFERENCES

1. Wang X, Han Q, Cornett J, Escort E, Zhang J. SU-E-I-55: cumulative radiation exposure and cancer risk estimates in pediatric hydrocephalus patients undergoing repeat or multiple CT. *Med Phys.* 2012;39(6Part4):3637.
2. Dobson GM, Dalton AK, Nicholson CL, Jenkins AJ, Mitchell PB, Cowie CJA. CT scan exposure in children with ventriculo-peritoneal shunts: single centre experience and review of the literature. *Childs Nerv Syst.* 2020;36(3):591-599.
3. Koral K, Blackburn T, Bailey AA, Koral KM, Anderson J. Strengthening the argument for rapid brain MR imaging: estimation of reduction in lifetime attributable risk of developing fatal cancer in children with shunted hydrocephalus by instituting a rapid brain MR imaging protocol in lieu of Head CT. *AJNR Am J Neuroradiol.* 2012;33(10):1851-1854.
4. Mandiwanza T, Saidlear C, Caird J, Crimmins D. The open fontanelle: a window to less radiation. *Childs Nerv Syst.* 2013;29(7):1177-1181.
5. Najjar A, Denault AY, Bojanowski MW. Bedside transcranial sonography monitoring in a patient with hydrocephalus post subarachnoid hemorrhage. *Crit Ultrasound J.* 2017;9(1):17.
6. Lee RP, Meggyesy M, Ahn J, et al. First experience with postoperative transcranial ultrasound through sonolucent burr hole covers in adult hydrocephalus patients. *Neurosurgery.* 2023;92(2):382-390.
7. Shay T, Mitchell KA, Belzberg M, et al. Translucent customized cranial implants made of clear polymethylmethacrylate: an early outcome analysis of 55 consecutive cranioplasty cases. *Ann Plast Surg.* 2020;85(6):e27-e36.
8. Belzberg M, Shalom NB, Lu A, et al. Transcranioplasty ultrasound through a sonolucent cranial implant made of polymethyl methacrylate: phantom study comparing ultrasound, computed tomography, and magnetic resonance imaging. *J Craniofac Surg.* 2019;30(7):e626-e629.
9. Belzberg M, Shalom NB, Yuhanna E, et al. Sonolucent cranial implants: cadaveric study and clinical findings supporting diagnostic and therapeutic transcranioplasty ultrasound. *J Craniofac Surg.* 2019;30(5):1456-1461.
10. González-Bonet LG. Spontaneous cranial bone regeneration after a craniectomy in an adult. *World Neurosurg.* 2021;147:67-69.
11. Debnath S, Yallowitz AR, McCormick J, et al. Discovery of a periosteal stem cell mediating intramembranous bone formation. *Nature.* 2018;562(7725):133-139.
12. Gosain AK, Gosain SA, Sweeney WM, Song LS, Amarante MTJ. Regulation of osteogenesis and survival within bone grafts to the calvaria: the effect of the dura versus the pericranium. *Plast Reconstr Surg.* 2011;128(1):85-94.
13. Gosain AK, Santoro TD, Song LS, Capel CC, Sudhakar PV, Matloub HS. Osteogenesis in calvarial defects: contribution of the dura, the pericranium, and the surrounding bone in adult versus infant animals. *Plast Reconstr Surg.* 2003;112(2):515-527.
14. Hämmerle CH, Schmid J, Lang NP, Olah AJ. Temporal dynamics of healing in rabbit cranial defects using guided bone regeneration. *J Oral Maxillofac Surg.* 1995;53(2):167-174.
15. Spotnitz WD. Fibrin sealant: the only approved hemostat, sealant, and adhesive—a laboratory and clinical perspective. *ISRN Surg.* 2014;2014:203943.
16. Flores AR, Srinivasan VM, Seeley J, Huggins C, Kan P, Burkhardt JK. Safety, feasibility, and patient-rated outcome of sonolucent cranioplasty in extracranial-intracranial bypass surgery to allow for transcranioplasty ultrasound assessment. *World Neurosurg.* 2020;144:e277-e284.
17. Salem MM, Ravindran K, Hoang AN, et al. Sonolucent cranioplasty in extracranial to intracranial bypass surgery: early multicenter experience of 44 cases. *Oper Neurosurg.* 2023;25(1):20-27.
18. Del Bene M, Raspagliesi L, Carone G, et al. Cranial sonolucent prosthesis: a window of opportunity for neuro-oncology (and neuro-surgery). *J Neurooncol.* 2022;156(3):529-540.
19. O'Malley GR, Jr, Cassimatis ND, Maggio J, Patel P, Patel NV. Sonolucent cranial implants: a window into the future of management of neurosurgical patients? A systematic review and cost analysis. *World Neurosurg.* 2024;181:e848-e855.

Acknowledgments

Author Contributions: Albert Antar, BS—Contributed to the design of the study, data collection, and analysis. Drafted the manuscript and provided critical revisions. Ryan P. Lee, MD—Conceptualized the study, interpreted the data, and revised the article. Shahab Aldin Sattari, MD—Conducted data analysis and manuscript revision. Michael Meggyesy, MD—Interpreted data and revised the manuscript. Jheesoo Ahn, BSN—Conceptualized the study and interpreted data. Carly Weber-Levine, MS—Drafted the manuscript and analyzed data. Kelly Jiang, MS—Drafted the manuscript and analyzed data. Judy Huang, MD—Provided oversight of the study design and implementation. Contributed to the interpretation of results and critical revision of the manuscript. Mark Luciano, MD, PhD—Served as the principal investigator, overseeing all aspects of the study. Contributed to the study design, data interpretation, and provided final approval of the manuscript.